Two-Photon Correlations in Atomic Transitions*

Edward S. Fry
Department of Physics, Texas A&M University, College Station, Texas 77843
(Received 22 January 1973)

A general formula is derived for two-photon coincidence rates. The result obtained is a function of the orientation of linear polarizers, of the solid angles subtended, and of the relative position of the photon detectors. It applies to both cascade emissions and resonance flourescence when the transitions are of electric dipole type. Allowance is made for anisotropic initial-state populations. It is shown that a single parameter describes the atomic transition when the initial states are isotropically populated. This parameter is found to have a particularly simple form, even when the nuclear spin is nonzero. It is the product of two Racah coefficients and an E coefficient defined here. Tables of the required Racah and E coefficients are provided so that this parameter can be easily determined when the states in the transitions have J values 0, 1, 2, 3, 4, 1/2, 3/2, 5/2, 7/2, or 9/2, and when the nuclear spin is 0, 1, 1/2, 3/2, 5/2, 7/2, or 9/2. Experiments to test hidden-variable theories which are possible in view of these results are discussed. Experiments to determine the effective quantum efficiency of photon detectors using these results are described.

I. INTRODUCTION

Coincidence observation of optical photons from an atomic cascade can be an extremely powerful experimental technique. However, owing to a lack of good single-photon detectors and the associated fast electronics, such experiments have been extraordinarily difficult and have not seen widespread use. The situation is changing. Recent advances in photomultiplier-tube technology have resulted in the production of fast, low-noise detectors with relatively high efficiencies. These are well suited to single-photon counting techniques. Together with the modern electronics available, they are increasing the importance of coincidence experiments in atomic physics. Thus a need has arisen for the predictions of two-photon coincidence rates which are derived here.

Some of the valuable results which can be obtained from coincidence experiments have already been pointed out by several authors.[1-5] These include: determination of excited-state lifetimes and g values, branching ratios, absolute quantum efficiencies and source strengths, and experimental tests of local hidden variables. Recent successful experiments include those reviewed by Camhy-Val and Dumont[6] as well as the important experiment of Freedman and Clauser.[7] The analogous coincidence techniques have, of course, been used extensively in nuclear physics and have yielded an abundance of useful information.

The theory of the angular correlations of nuclear emissions has been treated extensively in the literature. Good review articles containing extensive bibliographies are those of Devons and Goldfarb,[8] and Frauenfelder and Steffen.[9] Horne[10] has recently determined the coincidence rates for two specific atomic cascades, including solid angle and polarization effects. A general formula including the effects of solid angle, plane polarization, hyperfine structure, and anisotropic initial-state populations is evaluated here. The parameter describing transitions with isotropic initial-state populations is calculated for many transitions which might be experimentally observed. It is given in tabular form. Effects of nuclear spins from 0 to $\frac{9}{2}$ have been included. The results are applicable to both atomic cascade, and resonance fluorescence experiments.

Possible local hidden variable tests of the type suggested by Clauser *et al.*[2] are discussed. As suggested by Holt,[11] it is found that transitions in atoms with nonzero nuclear spin are unsuitable for such tests.

A technique by which the effective quantum efficiency of photon detectors can be measured is described. The important consideration in such measurements is the anisotropy in the direction of emission of the second photon with respect to that of the first. This is not a minor effect; it can, for example, produce solid angle factors which differ from those for isotropic emissions by as much as 50% (e.g., the 0-1-0 case). Finally, applications to resonance fluorescence experiments, and to the determination of branching ratios are discussed.

II. DERIVATION OF GENERAL RESULT

Figure 1 shows the typical angular-correlation experiment to be studied here. Two photon detectors face the origin with an angle θ_s between their axes. They subtend cones at the origin of half-angles Θ_i. Each detector has a linear polar-

izer and a wavelength filter in front of it. An excited atom in a source at the origin emits two photons in succession. We ask for the coincidence rate—i.e., for the relative probability that both photons will be detected. It will be assumed that the dimensions of the source are much less than the distance to the detectors.

Consider the excited atom to be in a state of total electron angular momentum J_i and to have a nuclear spin I. It decays by electric dipole transitions through an intermediate state J to a final state J_f emitting the two photons. This will be referred to as a $(J_i\text{-}J\text{-}J_f)$ transition. Suitable basis vectors for describing the angular dependence of the atomic states are z-component angular momentum eigenstates, $|JFm\rangle$. Here $\vec{F}=\vec{I}+\vec{J}$ is the total angular momentum of the atom, and m is the magnetic quantum number in the F representation. The two photons are represented as plane waves whose directions of travel are $\vec{k}_1$ and $\vec{k}_2$, respectively, and whose helicities, ±1, are denoted by σ_1 and σ_2, respectively, Detector 1 sees only photon 1 and detector 2 sees only photon 2. By generalizing the methods described by Horne,[10] or Frauenfelder and Steffen,[9] it is easily shown (see Appendix A) that the formal result for the polarized coincidence rate, including hyperfine effects, is

$$S \propto \int d\Omega_1 \int d\Omega_2 \sum_{\sigma_1,\sigma_1',\sigma_2,\sigma_2'} \langle\sigma_1'|\epsilon(1)|\sigma_1\rangle\langle\sigma_2'|\epsilon(2)|\sigma_2\rangle \sum_{\substack{F_i,m_i,F_f,m_f \\ F,m,m'}} (-1)^{m+m'} P(F_i,m_i)(2F+1)^2$$
$$\times C(F1F_i;m,m_i-m)C(F1F_i;m',m_i-m')C(F1F_f;m,m_f-m)$$
$$\times C(F1F_f;m',m_f-m')W^2(J_iJF_iF;1I)W^2(J_fJF_fF;1I)D^1_{\sigma_1,m_i-m}(k_1\to z)$$
$$\times D^{1*}_{\sigma_1',m_i-m'}(k_1\to z)D^1_{\sigma_2,m-m_f}(k_2\to z)D^{1*}_{\sigma_2',m'-m_f}(k_2\to z), \qquad (1)$$

where the following hold:

The integrations are over the solid angles subtended by the respective detectors. $D^1_{\sigma_1,m_i-m}(k_1\to z)$ are elements of the three-dimensional rotation matrix that rotates the coordinate system, $O_{x_1y_1,k_1}$, associated with the $\vec{k}_1$ propagation direction into a fixed laboratory coordinate system, O_{xyz}; see Fig. 2; similarly for the other D's. $\langle\sigma_1'|\epsilon(1)|\sigma_1\rangle$ are the matrix elements of the polarizer efficiency matrix for the first photon; similarly for the second photon. $P(F_i,m_i)$ is the relative population of the initial state F_i whose magnetic quantum number with respect to the laboratory z axis is m_i. (Only diagonal density matrices for the initial state are considered.) $C(F1F_i;m,m_i-m)$, etc., are Clebsch-Gordan coefficients. $W(J_iJF_iF_i;1I)$, etc., are Racah coefficients. These are introduced when the F dependence is taken out of the "reduced" matrix elements. The convention chosen for the states $|\pm1\rangle$ in terms of basis states along the x_i, y_i axes is respectively $\mp(\hat{e}_x \pm i\hat{e}_y)/2^{1/2}$ where $\hat{e}_x$ and $\hat{e}_y$ are unit vectors along the x_i and y_i axes.[12] This same convention must also be used in determining the efficiency matrices.[13] Finally, the conventions used for the Clebsch-Gordan and Racah coefficients and for the rotation matrices are those of Rose.[14]

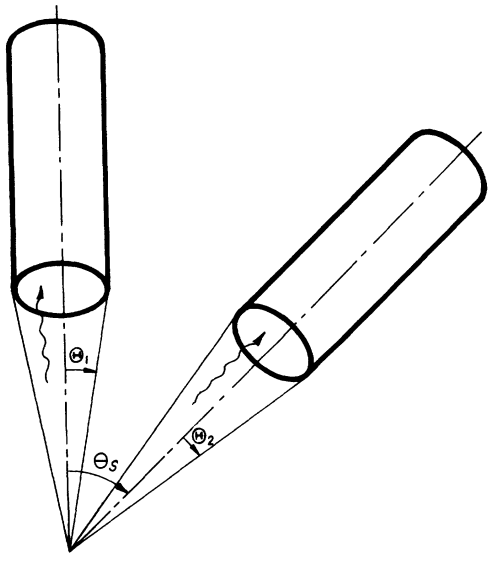

FIG. 1. Experimental configuration. The angle between the detector axes is θ_s. The half-angles of the cones subtended by the detectors are, respectively, Θ_1 and Θ_2.

In deriving Eq. (1) the natural width of the atomic states was assumed to be much less than the hyperfine-structure splitting. Under this condition the wavelengths of the emitted photons can be measured, and the F value of the intermediate state can be uniquely determined. Hence no interference between different F values can occur. In the summation over the intermediate-state F values in Eq. (1), the amplitudes were therefore squared before adding. The fact that in an actual experiment one might not accurately measure the wavelengths does not affect this result. It is the

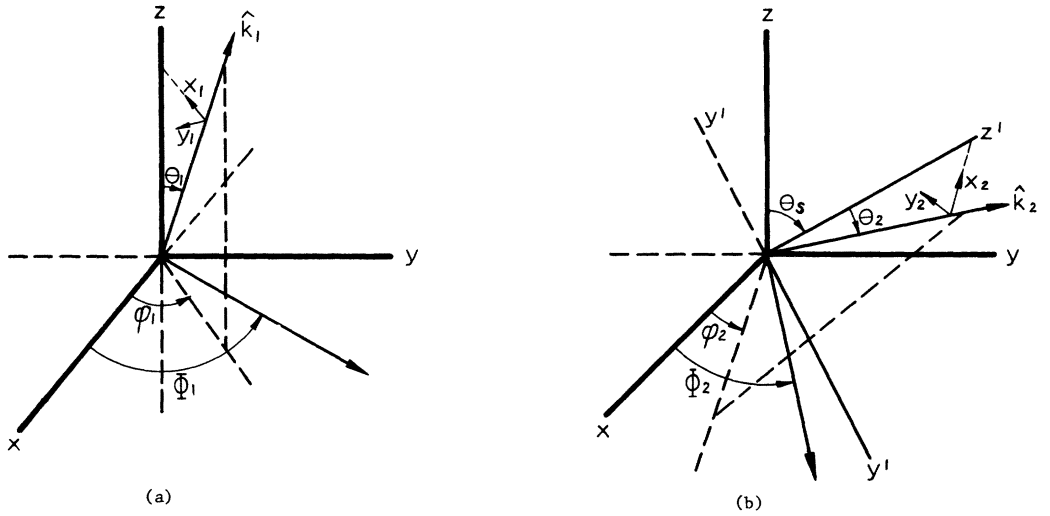

FIG. 2. (a) Geometry for the emission of the first photon: x_1 lies in the z-k_1 plane; θ_1 and ϕ_1 are the spherical coordinate angles of k_1 with respect to the x,y,z axes; Φ_1 is the angle between the x axis and the transmission axis of the first polarizer. (b) Geometry for the emission of the second photon: z' lies in the z-y plane and makes an angle θ_s with the z axis; x_2 lies in the z'-k_2 plane; θ_2 and ϕ_2 are the spherical coordinate angles of k_2 with respect to the x,y',z' axes; Φ_2 is the angle between the x axis and the transmission axis of the second polarizer; both ϕ_2 and Φ_2 are in the x-y' plane.

possibility of measuring the wavelength and the fact that it would yield a sharp value of F that destroys the interference.[9,15] Of course, for a given intermediate state F the summation over m is coherent. Conversely, when the hyperfine splitting is much less than the natural width of the levels, the sum over the intermediate-state F values must be coherent. When the initial state is isotropically populated and $I \neq 0$, this coherent sum is equivalent to the $I=0$ result. For physical reasons this is expected. A proof is given in Appendix B.

All the dependence on the atomic states which appears in Eq. (1) can be collected into coefficients denoted by B_n. Since all the angular dependence is in the rotation and efficiency matrices, it and the B_n's can be evaluated separately. Thus

$$S \propto \sum_{n=1}^{81} B_n \int d\Omega_1 \int d\Omega_2 \sum_{\sigma_1,\sigma_1',\sigma_2,\sigma_2'} \langle \sigma_1' | \epsilon(1) | \sigma_1 \rangle \times \langle \sigma_2' | \epsilon(2) | \sigma_2 \rangle D^1_{\sigma_1 n_1}(k_1 \to z) D^{1*}_{\sigma_1' n_2}(k_1 \to z) \times D^1_{\sigma_2 n_3}(k_2 \to z) D^{1*}_{\sigma_2' n_4}(k_2 \to z). \quad (2)$$

Here each subscript n_i can have only the values 0, ±1, and the subscript n is thus uniquely related to them by

$$n = 27(n_1+1) + 9(n_2+1) + 3(n_3+1) + n_4 + 2. \quad (3)$$

By comparing Eqs. (1) and (2) it is clear that

$$n_1 + n_3 = n_2 + n_4 . \quad (4)$$

Hence, the only acceptable values for n in Eq. (2) are

$$n = 1,\ 5,\ 9,\ 13,\ 17,\ 25,\ 29,\ 33,\ 37,\ 41,\ 45,\ 49,\ 53,\ 57,\ 65,\ 69,\ 73,\ 77,\ 81. \quad (5)$$

By setting

$$X(J_i F_i J F J_f F_f I) = (2F+1) W(J_i J F_i F; 1I) \times W(J_f J F_f F; 1I), \quad (6)$$

and by comparing Eqs. (1) and (2), the explicit formulas for the B_n can be obtained; several of these are

$$B_1 = \sum_{F_i,F_f,F,m} P(F_i, m-1)[C(F1F_i; m,-1) C(F1F_f; m,1) X(J_i F_i J F J_f F_f I)]^2, \quad (7)$$

$$B_5 = \sum_{F_i,F_f,F,m} P(F_i, m-1)[C(F1F_i; m,-1) C(F1F_f; m,0) X(J_i F_i J F J_f F_f I)]^2, \quad (8)$$

$$B_9 = \sum_{F_i,F_f,F,m} P(F_i, m-1)[C(F1F_i; m,-1) C(F1F_f; m,-1) X(J_i F_i J F J_f I)]^2, \quad (9)$$

$$B_{13}=\sum_{F_i,F_f,F,m} -P(F_i,\ m-1)C(F1F_i;\ m,-1)C(F1F_i;\ m-1,0)C(F1F_f;\ m,0)$$
$$\times C(F1F_f;\ m-1,1)X^2(J_i\,F_i\,JFJ_f\,F_f I), \tag{10}$$

$$B_{17}=\sum_{F_i,F_f,F,m} P(F_i,m-1)C(F1F_i;\ m,-1)C(F1F_i;\ m-1,0)C(F1F_f;m,-1)$$
$$\times C(F1F_f;\ m-1,0)X^2(J_i\,F_i\,JFJ_f\,F_f I), \tag{11}$$

$$B_{25}=\sum_{F_i,F_f,F,m} P(F_i,m-1)C(F1F_i;\ m,-1)C(F1F_i;\ m-2,1)C(F1F_f;\ m,-1)$$
$$\times C(F1F_f;\ m-2,1)X^2(J_i\,F_i\,JFJ_f\,F_f I), \tag{12}$$

$$B_{37}=\sum_{F_i,F_f,F,m} P(F_i,m)[C(F1F_i;\ m,0)C(F1F_f;\ m,1)X(J_i\,F_i\,JFJ_f\,F_f I)]^2, \tag{13}$$

$$B_{41}=\sum_{F_i,F_f,F,m} P(F_i,m)[C(F1F_i;\ m,0)C(F1F_f;\ m,0)X(J_iF_i\,JFJ_f\,F_f I)]^2. \tag{14}$$

Analogous formulas give the other B coefficients. By changing the summation index m these identities among them are found:

$$B_{29}=B_{13},\quad B_{33}=B_{17},\quad B_{57}=B_{25},\quad B_{65}=B_{49},\quad B_{69}=B_{53}. \tag{15}$$

The coincidence rate is now given by

$$S\propto\int d\Omega_1\int d\Omega_2\sum_{\sigma_1\sigma_1'\sigma_2\sigma_2'}\langle\sigma_1'|\epsilon(1)|\sigma\rangle\langle\sigma_2'|\epsilon(2)|\sigma_2\rangle[B_1 d_{-1,-1,-1,-1}+B_{81}d_{1,1,1,1}+B_5 d_{-1,-1,0,0}+B_{77}d_{1,1,0,0}$$
$$+B_9 d_{-1,-1,1,1}+B_{73}d_{1,1,-1,-1}+B_{13}(d_{-1,0,0,-1}+d_{0,-1,-1,0})$$
$$+B_{53}(d_{0,1,1,0}+d_{1,0,0,1})+B_{17}(d_{-1,0,1,0}+d_{0,-1,0,1})$$
$$+B_{49}(d_{0,1,0,-1}+d_{1,0,-1,0})+B_{25}(d_{-1,1,1,-1}+d_{1,-1,-1,1})$$
$$+B_{37}d_{0,0,-1,-1}+B_{45}d_{0,0,1,1}+B_{41}d_{0,0,0,0}], \tag{16}$$

where

$$d_{i,j,k,l}=D^1_{\sigma_1,i}(k_1\to z)D^{1*}_{\sigma_1',j}(k_1\to z)D^1_{\sigma_2,k}(k_2\to z)D^{1*}_{\sigma_2',l}(k_2\to z).$$

Using a Clebsch-Gordan identity, it is easily shown that if

$$P(F_i,m)=P(F_i,-m) \tag{17}$$

then all of the B's are given by the eight B's defined in Eqs. (7)–(14):

$$B_{81}=B_1,\quad B_{77}=B_5,\quad B_{73}=B_9,$$
$$B_{45}=B_{37},\quad B_{53}=B_{13},\quad B_{49}=B_{17}. \tag{18}$$

Equation (17) is satisfied for isotropic initial populations. It may also be satisfied, for example, if the initial state is populated by absorption of linear polarized light. B coefficients for several transitions have been evaluated and are given in Table I. The proportionality has been adjusted so that these are integers. The transitions with isotropic populations in the initial state are more easily studied in terms of the A coefficient which is defined later by Eqs. (37) and (40); hence, only three of these are given in Table I.

Further evaluation of Eq. (16) requires specification of the geometry; see Fig. 1 and Figs. 2(a) and 2(b). The emitting atom is at the origin. Detector 1 is on the laboratory $+z$ axis. Detector 2 lies on an axis z' which is at an angle θ_s to the laboratory $+z$ axis. The laboratory x and y axes are defined so that detector 2 lies in the laboratory y-z plane. Detector 1 (2) has a circular aperture subtending a cone at the origin of half-angle Θ_1 (Θ_2). The propagation direction $\vec{k}_1$ ($\vec{k}_2$) makes an angle θ_1 (θ_2) with the $+z$ (z') axis. The coordinate system $O_{x_1y_1k_1}$ ($O_{x_2y_2k_2}$) is defined by taking x_1 (x_2) to point toward the z (z') axis. The transmission axis of polarizer 1 (2) makes an angle Φ_1 (Φ_2) with the laboratory x axis. The angle between the x_1 (x_2) linear polarization of photon 1 (2) and the transmission axis of polarizer 1 (2) is $\Phi_1-\phi_1$ ($\Phi_2-\phi_2$).

First, consider the efficiency matrices. The matrix of a linear polarizer in basis states parallel and perpendicular to its transmission axis is

TABLE I. Some typical B coefficients. The proportionality constant has been adjusted for each transition so that the B's are integers. The nuclear spin is zero, $I=0$, in all transitions considered here. The function $F(0)$ defined by Eq. (46a) has also been included.

Transition J_i-J-J_f	Initial-state populations[a]	B_1	B_5	B_9	B_{25}	B_{37}	B_{41}	B_{45}	B_{73}	B_{77}	B_{81}	$F(0)$
0-1-0	(I)	0	0	1	1	0	1	0	1	0	0	1.000
1-1-0	(I)	0	1	1	−1	1	0	1	1	1	0	−1.000
$\frac{3}{2}$-$\frac{3}{2}$-$\frac{1}{2}$	(I)	3	14	13	−12	14	2	14	13	14	3	−0.750
1-1-0	(II)	0	1	1	−1	1	0	0	1	0	0	−1.000
1-1-0	(III)	0	1	0	0	1	0	1	0	1	0	0.000
1-1-0	(IV)	0	0	1	−1	0	0	0	1	0	0	−1.000
1-1-1	(IV)	0	1	1	1	0	0	0	1	1	0	1.000
1-1-2	(IV)	6	3	1	−1	0	0	0	1	3	6	−0.143
1-2-1	(IV)	0	9	9	9	4	16	4	9	9	0	1.000
1-2-2	(IV)	2	1	3	−3	4	0	4	3	1	2	−0.600
2-1-0	(V)	0	9	4	4	9	16	9	4	9	0	1.000
2-1-1	(V)	9	4	13	−4	25	18	25	13	4	9	−0.182
2-1-2	(V)	51	48	31	4	111	118	111	31	48	51	0.049
2-2-1	(V)	1	8	9	−8	1	2	1	9	8	1	−0.800
$\frac{1}{2}$-$\frac{1}{2}$-$\frac{1}{2}$	(VI)	0	2	4	0	2	1	0	0	0	0	0.000
$\frac{1}{2}$-$\frac{3}{2}$-$\frac{1}{2}$	(VI)	0	2	1	3	2	4	0	9	0	0	0.600
$\frac{1}{2}$-$\frac{3}{2}$-$\frac{3}{2}$	(VI)	6	1	8	−12	16	2	12	18	27	0	−0.750
$\frac{3}{2}$-$\frac{1}{2}$-$\frac{1}{2}$	(VII)	0	1	2	0	2	2	2	2	1	0	0.000
$\frac{3}{2}$-$\frac{1}{2}$-$\frac{3}{2}$	(VII)	3	2	1	0	8	8	8	1	2	3	0.000
$\frac{3}{2}$-$\frac{3}{2}$-$\frac{1}{2}$	(VII)	0	16	26	−24	1	4	1	26	16	0	−0.923
$\frac{3}{2}$-$\frac{3}{2}$-$\frac{3}{2}$	(VII)	24	31	50	48	7	1	7	50	31	24	0.649
$\frac{3}{2}$-$\frac{3}{2}$-$\frac{5}{2}$	(VII)	36	24	10	−8	3	4	3	10	24	36	−0.174
$\frac{3}{2}$-$\frac{5}{2}$-$\frac{3}{2}$	(VII)	1	14	15	12	8	24	8	15	14	1	0.750
$\frac{3}{2}$-$\frac{5}{2}$-$\frac{5}{2}$	(VII)	36	19	50	−48	68	4	68	50	19	36	−0.558
$\frac{5}{2}$-$\frac{3}{2}$-$\frac{1}{2}$	(VIII)	2	7	3	3	7	12	7	3	7	2	0.600

[a] (I): isotropic; (II): $P(1,-1)=P(1,0)=1$, $P(1,1)=0$; (III): $P(1,\pm1)=1$, $P(1,0)=0$;
(IV): $P(1,\pm1)=0$, $P(1,0)=1$; (V): $P(2,\pm2)=0$, $P(2,\pm1)=3$, $P(2,0)=4$;
(VI): $P(\frac{1}{2},\frac{1}{2})=0$, $P(\frac{1}{2},-\frac{1}{2})=1$; (VII): $P(\frac{3}{2},\pm\frac{3}{2})=0$, $P(\frac{3}{2},\pm\frac{1}{2})=1$;
(VIII): $P(\frac{5}{2},\pm\frac{5}{2})=0$, $P(\frac{5}{2},\pm\frac{3}{2})=2$, $P(\frac{5}{2},\pm\frac{1}{2})=3$.

$$\epsilon=\begin{pmatrix}\epsilon_M & 0\\ 0 & \epsilon_m\end{pmatrix}, \tag{19}$$

where ϵ_M and ϵ_m are the ratios of transmitted to incident light intensity polarized parallel and perpendicular, respectively, to the transmission axis. For a perfect linear polarizer $\epsilon_M=1$ and $\epsilon_m=0$. If the polarizer is removed $\epsilon_M=\epsilon_m=1$. To obtain the elements of the efficiency matrix, $\langle\sigma_1'|\epsilon(1)|\sigma_1\rangle$, required in Eqs. (18), we must first transform Eq. (19) to basis states along the x_1, y_1 axes and then transform it to circular polarization basis states using the convention employed in deriving Eq. (1). These elementary transformations give

$$\langle\sigma_1'|\epsilon(1)|\sigma_1\rangle=\begin{pmatrix}a_1 & -b_1 e^{-2i(\Phi_1-\phi_1)}\\ -b_1 e^{2i(\Phi_1-\phi_1)} & a_1\end{pmatrix}. \tag{20}$$

Similarly, we have

$$\langle\sigma_2'|\epsilon(2)|\sigma_2\rangle=\begin{pmatrix}a_2 & -b_2 e^{-2i(\Phi_2-\phi_2)}\\ -b_2 e^{2i(\Phi_2-\phi_2)} & a_2\end{pmatrix}. \tag{21}$$

The coefficients a and b in these relations are given by

$$a_i=\tfrac{1}{2}[\epsilon_M(i)+\epsilon_m(i)], \qquad b_i=\tfrac{1}{2}[\epsilon_M(i)-\epsilon_m(i)]. \tag{22}$$

For a perfect polarizer $a_i=b_i=\frac{1}{2}$. Removal of a polarizer corresponds to $a_i=1$, $b_i=0$.

Now, consider the rotation matrices. For $D^1(k_1\to z)$ the Euler angles (α,β,γ) obtained from Fig. 2(a) are $(0,\theta_1,\pi-\phi_1)$. Thus, we have

$$D^1(k_1\to z)=\begin{pmatrix}-e^{i\phi_1}\cos^2(\frac{1}{2}\theta_1) & 2^{-1/2}\sin\theta_1 & -e^{-i\phi_1}\sin^2(\frac{1}{2}\theta_1)\\ -2^{-1/2}e^{i\phi_1}\sin\theta_1 & \cos\theta_1 & 2^{-1/2}e^{-i\phi_1}\sin\theta_1\\ -e^{i\phi_1}\sin^2(\frac{1}{2}\theta_1) & 2^{-1/2}\sin\theta_1 & -e^{-i\phi_1}\cos^2(\frac{1}{2}\theta_1)\end{pmatrix}. \tag{23}$$

The matrix $D^1(k_2 \to z)$ is obtained by means of a rotation $k_2 \to z'$ followed by a rotation $z' \to z$,

$$D^1(k_2 \to z) = D^1(k_2 \to z')D^1(z' \to z). \tag{24}$$

From Fig. 2(b) the Euler angles for the successive rotations are $(0, \theta_2, \pi - \phi_2)$ and $(-\frac{1}{2}\pi, \theta_s, \frac{1}{2}\pi)$, respectively. $D^1(k_2 \to z)$ is then given by the matrix product

$$D^1(k_2 \to z) = \begin{pmatrix} -e^{i\phi_2}\cos^2(\frac{1}{2}\theta_2) & 2^{-1/2}\sin\theta_2 & -e^{-i\phi_2}\sin^2(\frac{1}{2}\theta_2) \\ -2^{-1/2}e^{i\phi_2}\sin\theta_2 & \cos\theta_2 & 2^{-1/2}e^{-i\phi_2}\sin\theta_2 \\ -e^{i\phi_2}\sin^2(\frac{1}{2}\theta_2) & 2^{-1/2}\sin\theta_2 & -e^{-i\phi_2}\cos^2(\frac{1}{2}\theta_2) \end{pmatrix}$$
$$\times \begin{pmatrix} \cos^2(\frac{1}{2}\theta_s) & -2^{-1/2}i\sin\theta_s & -\sin^2(\frac{1}{2}\theta_s) \\ -2^{-1/2}i\sin\theta_s & \cos\theta_s & -2^{-1/2}i\sin\theta_s \\ -\sin^2(\frac{1}{2}\theta_s) & -2^{-1/2}i\sin\theta_s & \cos^2(\frac{1}{2}\theta_s) \end{pmatrix}. \tag{25}$$

Equation (16) is to be evaluated using these rotation and efficiency matrices. There are 16 terms in the sum over the σ's and there are 19 functions $d_{i,j,k,l}$; hence there are 304 terms to be evaluated. If the integrations $(0 \to 2\pi)$ over ϕ_1 and ϕ_2 are simultaneously performed, it is quickly seen that most of these terms integrate to zero. The remaining 80 terms give

$$\begin{aligned} S \propto \int_0^{\Theta_1} \sin\theta_1 d\theta_1 \int_0^{\Theta_2} \sin\theta_2 d\theta_2 \{ & a_1a_2[(B_1 + B_9 + B_{73} + B_{81})g(\theta_1) + (B_{37} + B_{45})\sin^2\theta_1][2g(\theta_2)g(\theta_s) + \sin^2\theta_2\sin^2\theta_s] \\ & + 2a_1a_2[(B_5 + B_{77})g(\theta_1) + B_{41}\sin^2\theta_1][g(\theta_2)\sin^2\theta_s + \sin^2\theta_2\cos^2\theta_s] \\ & + a_1b_2[(B_1 + B_9 - 2B_5 - 2B_{77} + B_{73} + B_{81})g(\theta_1) - (2B_{41} - B_{37} - B_{45})\sin^2\theta_1] \\ & \times \cos^4(\tfrac{1}{2}\theta_2)\sin^2\theta_s\cos 2\Phi_2 + 2a_2b_1B_{25}[g(\theta_2) - \sin^2\theta_2]\cos^4(\tfrac{1}{2}\theta_1)\sin^2\theta_s\cos 2\Phi_1 \\ & + 4b_1b_2B_{25}\cos^4(\tfrac{1}{2}\theta_1)\cos^4(\tfrac{1}{2}\theta_2)[\cos^4(\tfrac{1}{2}\theta_s)\cos 2(\Phi_1 - \Phi_2) + \sin^4(\tfrac{1}{2}\theta_s)\cos 2(\Phi_1 + \Phi_2)]\}, \end{aligned} \tag{26}$$

It has been implicitly assumed that the detector has uniform sensitivity across its aperture. This greatly simplified the problem for the integrations over ϕ_1 and ϕ_2. However, if the sensitivity has a nonuniformity which is symmetric about the detector axis, then the ϕ_i integrations are unchanged. The nonuniform sensitivity $s_i(\theta_i)$, being a function only of θ_i, can be inserted into the integrals in Eq. (26) without seriously complicating the problem.

If we define the solid angle functions

$$\begin{aligned} G(\Theta) &= \int_0^{\Theta} s(\theta)\sin\theta d\theta, \\ H(\Theta) &= \tfrac{1}{4}\int_0^{\Theta} s(\theta)(3\cos^2\theta - 1)\sin\theta d\theta, \\ J(\Theta) &= \tfrac{3}{2}\int_0^{\Theta} s(\theta)\cos^4(\tfrac{1}{2}\theta)\sin\theta d\theta, \end{aligned} \tag{27}$$

then all the integrals in Eq. (26) can be given in terms of them. If $s(\theta) = 1$, the solid angle functions become

$$\begin{aligned} G_0(\Theta) &= 1 - \cos\Theta, \\ H_0(\Theta) &= \tfrac{1}{4}\sin^2\Theta\cos\Theta, \\ J_0(\Theta) &= \tfrac{1}{2}(1 - \cos\Theta) + \tfrac{1}{8}\sin^2\Theta\cos\Theta + \tfrac{3}{8}\sin^2\Theta. \end{aligned} \tag{28}$$

Performing the integrations in Eq. (26) and rearranging terms gives

$$\begin{aligned} S \propto & 2a_1a_2[\beta_1 G(\Theta_1) + \beta_2 H(\Theta_1)]G(\Theta_2) + a_1a_2[\beta_3 G(\Theta_1) + \beta_4 H(\Theta_1)]H(\Theta_2)(3\cos^2\theta_s - 1) \\ & + a_1b_2[\beta_3 G(\Theta_1) + \beta_4 H(\Theta_1)]J(\Theta_2)\sin^2\theta_s\cos 2\Phi_2 + 6a_2b_1B_{25}J(\Theta_1)H(\Theta_2)\sin^2\theta_s\cos 2\Phi_1 \\ & + 4b_1b_2B_{25}J(\Theta_1)J(\Theta_2)[\cos^4(\tfrac{1}{2}\theta_s)\cos 2(\Phi_1 - \Phi_2) + \sin^4(\tfrac{1}{2}\theta_s)\cos 2(\Phi_1 + \Phi_2)], \end{aligned} \tag{29}$$

where

$$\beta_1 = B_1 + B_5 + B_9 + B_{37} + B_{41} + B_{45} + B_{73} + B_{77} + B_{81}, \quad \beta_2 = B_1 + B_5 + B_9 - 2B_{37} - 2B_{41} - 2B_{45} + B_{73} + B_{77} + B_{81},$$
$$\beta_3 = B_1 - 2B_5 + B_9 + B_{37} - 2B_{41} + B_{45} + B_{73} - 2B_{77} + B_{81}, \quad \beta_4 = B_1 - 2B_5 + B_9 - 2B_{37} + 4B_{41} - 2B_{45} + B_{73} - 2B_{77} + B_{81}. \tag{30}$$

The only restriction on the application of Eq. (29) is that detector 1 must be placed on the laboratory z axis. This is the symmetry axis with respect to which the anisotropic initial-state populations were given. The coincidence rate for detector 2 on the z axis and detector 1 at an angle θ_s is similar to Eq. (29). It can be obtained from Eq. (29) by interchanging β_2 and β_3, and by interchanging the subscripts 1 and 2 on a, b, Θ, and Φ. It should also be noted that if the polarizers are removed ($b_1 = b_2 = 0$), then Eq. (29) reduces to the result obtained by summing incoherently over the intermediate-state m values. This is, of course, the expected result.[9]

For isotropic populations in the initial state $[P(F_i, m_i) = \text{const}]$, Eq. (29) is considerably simplified. Since Eq. (17) and hence Eqs. (18) are satisfied, we begin with the eight B coefficients given by Eqs. (7)–(14). For isotropic populations there are five relations between these and hence only three of them are linearly independent. The five relations are found by setting $P(F_i, m) = 1$ and first explicitly evaluating the sum over m in each of them. For example, consider $\overline{B}_5$ (i.e., B_5 with isotropic initial-state populations):

$$\overline{B}_5 = \sum_{F_i, F_f, F} X^2 \sum_m C(F1F_f; m, 0) C(F1F_f; m, 0) \times C(F1F_i; m, -1) C(F1F_i; m, -1). \tag{31}$$

Using relations between the Racah coefficients,[14] and then explicitly evaluating the sum over m gives

$$\overline{B}_5 = \sum_{F_i, F_f, F} X^2 (-1)^{F_i + F_f + 1} (2F_f + 1)(2F_i + 1) \times \sum_{r=0}^{2} W(F1F1; F_f r) W(F1F1; F_i r) \times C(11r; 0, 0) C(11r; -1, 1). \tag{32}$$

Recalling the definition of X from Eq. (6) and using a sum rule for the Racah coefficients due to Biedenharn,[14] the sums over F_i and F_f may be evaluated giving

$$\overline{B}_5 = -\sum_{r=0}^{2} \sum_F (2F + 1)^2 W(1rJ_f J; 1J) W(1rJ_i J; 1J) \times W^2(FFJJ; rI) C(11r; 0, 0) C(11r; -1, 1). \tag{33}$$

Evaluating $\overline{B}_{37}$ in the same way gives an identical result; hence

$$\overline{B}_{37} = \overline{B}_5. \tag{34}$$

The remaining four relations can be found by expressing the other B's in a form analogous to Eq. (33) and comparing the Clebsch-Gordan coefficients that appear in the sum over r. Taking $\overline{B}_1$, $\overline{B}_5$, and $\overline{B}_9$ as the independent B's, these relations are

$$\overline{B}_{13} = \overline{B}_1 - \overline{B}_5, \quad \overline{B}_{17} = \overline{B}_5 - \overline{B}_9, \quad \overline{B}_{25} = \overline{B}_1 + \overline{B}_9 - 2\overline{B}_5, \quad \overline{B}_{41} = \overline{B}_1 + \overline{B}_9 - \overline{B}_5. \tag{35}$$

Using Eqs. (18), (34), and (35) in Eq. (29), the coincidence rate becomes

$$S \propto 3a_1a_2 G(\Theta_1) G(\Theta_2) + A\{6a_1a_2 H(\Theta_1) H(\Theta_2)(3\cos^2\theta_s - 1) + 6a_1b_2 H(\Theta_1) J(\Theta_2) \sin^2\theta_s \cos 2\Phi_2 + 6b_1a_2 J(\Theta_1) H(\Theta_2) \sin^2\theta_s \cos 2\Phi_1 + 4b_1b_2 J(\Theta_1) J(\Theta_2) [\cos^4(\tfrac{1}{2}\theta_s) \cos 2(\Phi_1 - \Phi_2) + \sin^4(\tfrac{1}{2}\theta_s) \cos 2(\Phi_1 + \Phi_2)]\}, \tag{36}$$

where

$$A = (\overline{B}_1 - 2\overline{B}_5 + \overline{B}_9)/2(\overline{B}_1 + \overline{B}_5 + \overline{B}_9). \tag{37}$$

We may put A in a different form which facilitates evaluation. Using Eq. (33) and the analogous expressions for $\overline{B}_1$ and $\overline{B}_9$, we find

$$\overline{B}_1 - 2\overline{B}_5 + \overline{B}_9 = W(12J_i J; 1J) W(12J_f J; 1J) \times \sum_F (2F + 1)^2 W^2(FFJJ; 2I) \tag{38}$$

and

$$\overline{B}_1 + \overline{B}_5 + \overline{B}_9 = (2I + 1)/3(2J + 1). \tag{39}$$

Hence, the coefficient A is given by

$$A = W(12J_i J; 1J) W(12J_f J; 1J) E(J, I), \tag{40}$$

where

$$E(J, I) = \tfrac{3}{2}[(2J + 1)/(2I + 1)] \sum_F (2F + 1)^2 W^2(FFJJ; 2I), \tag{41}$$

TABLE II. $E(J,I)$.

$J=$ \ $I=$	0	$\frac{1}{2}$	1	$\frac{3}{2}$	$\frac{5}{2}$	$\frac{7}{2}$	$\frac{9}{2}$
0	0	0	0	0	0	0	0
1	9/2	3/2	5/4	111/100	349/350	107/112	2573/2750
2	15/2	57/10	71/20	405/196	545/294	73 369/43 120	570 737/350 350
3	21/2	129/14	825/112	45 011/8400	5273/1925	31 247/12 012	11 824/4875
4	27/2	25/2	13 163/1200	21 583 993/2 371 600	10 369 101/1 926 925	2 044 571/592 900	548 769 769/163 788 625
$\frac{1}{2}$	0	0	0	0	0	0	0
$\frac{3}{2}$	6/1	15/4	44/25	81/50	1957/1400	1837/1400	13 991/11 000
$\frac{5}{2}$	9/1	15/2	6709/1225	139 341/39 200	34 669/14 700	459 297/215 600	1 007 037/500 500
$\frac{7}{2}$	12/1	87/8	4055/441	106 333/14 700	415 383/107 800	65 125/21 021	17 250 151/6 006 000
$\frac{9}{2}$	15/1	141/10	69 143/5445	127 045/11 616	313 155/44 044	22 955 629/5 285 280	30 801 271/8 022 300

and F ranges over all values for which the Racah coefficient is nonzero.

Thus, for isotropic initial-state populations, the dependence of the coincidence rate on the atomic system is contained in the single coefficient A given by Eq. (40). The function $E(J,I)$ required for its determination has been evaluated as a rational fraction for most J values and nuclear spins which might arise in experimentally observed atomic transitions. It is tabulated in Table II. For convenience the required Racah coefficient has been tabulated in Table III. Values of A for some common transitions are given in Table IV. The coefficient A, defined here, is identical to the A_{22} used by Frauenfelder and Steffen,[9] and it can be evaluated from their tables when $I=0$.

It is obvious from Eq. (40) that A is symmetric in the initial and final states. Hence the result for S in a $(J_f\text{-}J\text{-}J_i)$ transition will be identical to that in a $(J_i\text{-}J\text{-}J_f)$ transition. Note also that S, given by Eq. (36), is symmetric in the two detection systems—i.e., interchanging the subscripts 1 and 2 leaves S unchanged.

Finally, coincidence rates for the same transition, but with different nuclear spins can be compared using Eq. (36) directly. The fact that we have used $P(F_i, m_i)=1$ instead of a properly normalized $P(F_i, m_i)=[(2J_i+1)(2I+1)]^{-1}$ introduces no corrections for such a comparison. This is because the factor $(2I+1)^{-1}$ appearing in a normalized $P(F_i, m_i)$ has already been introduced into Eq. (36) through the factor $(\bar{B}_1+\bar{B}_5+\bar{B}_9)$ given by Eq. (39).

TABLE III. $W(12jJ;1J)$.

$J=$ \ $j=$	$J-1$	J	$J+1$
0	···	0	0
1	1/3	−1/6	1/30
2	$(21)^{1/2}/30$	$-(21)^{1/2}/30$	$(21)^{1/2}/105$
3	$(14)^{1/2}/35$	$-(14)^{1/2}/28$	$(14)^{1/2}/84$
4	$(462)^{1/2}/252$	$-(462)^{1/2}/180$	$(462)^{1/2}/495$
$\frac{1}{2}$	···	0	0
$\frac{3}{2}$	$(6)^{1/2}/12$	$-(6)^{1/2}/15$	$(6)^{1/2}/60$
$\frac{5}{2}$	$(14)^{1/2}/30$	$-4(14)^{1/2}/105$	$(14)^{1/2}/84$
$\frac{7}{2}$	$(7)^{1/2}/28$	$-(7)^{1/2}/21$	$(7)^{1/2}/60$
$\frac{9}{2}$	$(22)^{1/2}/60$	$-4(22)^{1/2}/165$	$(22)^{1/2}/110$

III. APPLICATIONS

A. Hidden Variables

In an experimental, hidden-variables, test of the type described by Clauser, *et al.*,[2] detector 1 is on the $+z$ axis and detector 2 is on the $-z$ axis. Hence $\theta_s=\pi$, the angle between the polarizer axes is $\phi=\Phi_1+\Phi_2$, and the coincidence rate from Eq. (29) becomes

$$S\propto a_1a_2[\beta_1G(\Theta_1)G(\Theta_2)+\beta_2H(\Theta_1)G(\Theta_2)+\beta_3G(\Theta_1)H(\Theta_2)+\beta_4H(\Theta_1)H(\Theta_2)]+2b_1b_2B_{25}J(\Theta_1)J(\Theta_2)\cos2\phi\,. \tag{42}$$

The coincidence rate with polarizers removed, S_0, is given by setting $b_1=b_2=0$ and $a_1=a_2=1$ in Eq. (42). For simplicity, we set $\Theta_1=\Theta_2=\Theta$; then the normalized coincidence rate is

$$S/S_0=a_1a_2+b_1b_2F(\Theta)\cos2\phi, \tag{43}$$

where

$$F(\Theta)=\frac{2B_{25}J^2(\Theta)}{\beta_1G^2(\Theta)+(\beta_2+\beta_3)G(\Theta)H(\Theta)+\beta_4H^2(\Theta)}\,. \tag{44}$$

For isotropic initial-state populations this is

$$\bar{F}(\Theta)=4AJ^2(\Theta)/[3G^2(\Theta)+12AH^2(\Theta)]. \quad (45)$$

For each case, in the limit $\Theta\to 0$ we have

$$F(0)=2B_{25}/(B_1+B_9+B_{73}+B_{81}), \quad (46a)$$

$$\bar{F}(0)=3A/(1+A). \quad (46b)$$

To simplify the relation between polarizer efficiency and detector solid angle, set $\epsilon_m(1)=\epsilon_m(2)=0$ and $\epsilon_M(1)=\epsilon_M(2)=\epsilon$. Then it can be shown[10] that the experimental test of hidden variables requires

$$\epsilon\geq 2/[1+2^{1/2}|F(\Theta)|]. \quad (47)$$

Now $|F(\Theta)|$ is a monotonic decreasing function of Θ; and since ϵ must be less than unity, the only possible cascades which can be used in these experiments are those for which

$$|F(0)|\geq 2^{-1/2}. \quad (48)$$

Values of $F(0)$ for some transitions are given in Tables I and IV.

Consider first the cascades in which the initial states are isotropically populated. Some of these are considered in Table IV. For a great many others $F(0)$ can be easily determined by evaluating A using Eq. (40) with the data in Tables II and III and then using Eq. (46b). Of all these cascades there are only five which satisfy Eq. (48). All have zero nuclear spin or equivalently have hyperfine-structure splittings which are much less than the natural width of the states—see Appendix B. They are (a) $(0-1-0)$, (b) $(1-1-0)$ or $(0-1-1)$, and (c) $(\frac{3}{2}-\frac{3}{2}-\frac{1}{2})$ or $(\frac{1}{2}-\frac{3}{2}-\frac{3}{2})$.

By manipulating the populations in the initial states, one can obtain any number of cascades which satisfy Eq. (48). One group of such cascades provides several feasible candidates for hidden-variable-type experiments. The initial states J_i of these cascades are populated by exciting them from states whose J value is J_i-1. The excitation mechanism is absorption of light which is plane polarized parallel to the z axis. Some cascades of this type are included in Table I. Those which satisfy Eq. (48) are

(d) $(1-1-0)$, $P(1,\pm1)=0$, $P(1,0)=1$;
(e) $(1-1-1)$, $P(1,\pm1)=0$, $P(1,0)=1$;
(f) $(1-2-1)$, $P(1,\pm1)=0$, $P(1,0)=1$;
(g) $(2-1-0)$, $P(2,\pm2)=0$, $P(2,\pm1)=3$, $P(2,0)=4$;
(h) $(2-2-1)$, $P(2,\pm2)=0$, $P(2,\pm1)=3$, $P(2,0)=4$;
(i) $(\frac{3}{2}-\frac{3}{2}-\frac{1}{2})$, $P(\frac{3}{2},\pm\frac{3}{2})=0$, $P(\frac{3}{2},\pm\frac{1}{2})=1$;
(j) $(\frac{3}{2}-\frac{5}{2}-\frac{3}{2})$, $P(\frac{3}{2},\pm\frac{3}{2})=0$, $P(\frac{3}{2},\pm\frac{1}{2})=1$.

TABLE IV. The A coefficient, defined only for isotropic populations in the initial state. The function $F(0)$ has also been included.

Transition J_i-J-J_f	I	A	$F(0)$	Transition J_i-J-J_f	I	A	$F(0)$
0-1-0	0	1/2	1.000	$\frac{1}{2}$-$\frac{1}{2}$-$\frac{1}{2}$	0	0	0.0
	$\frac{1}{2}$	1/6	0.429		$\frac{1}{2}$	0	0.0
	$\frac{3}{2}$	37/300	0.329		$\frac{3}{2}$	0	0.0
	$\frac{5}{2}$	349/3150	0.299		$\frac{5}{2}$	0	0.0
0-1-1	0	−1/4	−1.000	$\frac{1}{2}$-$\frac{1}{2}$-$\frac{3}{2}$	0	0	0.0
	$\frac{1}{2}$	−1/12	−0.273		$\frac{1}{2}$	0	0.0
	$\frac{3}{2}$	−37/600	−0.197		$\frac{3}{2}$	0	0.0
	$\frac{5}{2}$	−349/6300	−0.176		$\frac{5}{2}$	0	0.0
0-1-2	0	1/20	0.143	$\frac{1}{2}$-$\frac{3}{2}$-$\frac{1}{2}$	0	1/4	0.600
	$\frac{1}{2}$	1/60	0.049		$\frac{1}{2}$	5/32	0.405
	$\frac{3}{2}$	37/3000	0.037		$\frac{3}{2}$	27/400	0.190
	$\frac{5}{2}$	349/31 500	0.033		$\frac{5}{2}$	1957/33 600	0.165
1-0-1	0	0	0.0	$\frac{1}{2}$-$\frac{3}{2}$-$\frac{3}{2}$	0	−1/5	−0.750
	$\frac{1}{2}$	0	0.0		$\frac{1}{2}$	−1/8	−0.429
	$\frac{3}{2}$	0	0.0		$\frac{3}{2}$	−27/500	−0.171
	$\frac{5}{2}$	0	0.0		$\frac{5}{2}$	−1957/42 000	−0.147
1-1-1	0	1/8	0.333	$\frac{1}{2}$-$\frac{3}{2}$-$\frac{5}{2}$	0	1/20	0.143
	$\frac{1}{2}$	1/24	0.120		$\frac{1}{2}$	1/32	0.091
	$\frac{3}{2}$	37/1200	0.090		$\frac{3}{2}$	27/2000	0.040
	$\frac{5}{2}$	349/12 600	0.081		$\frac{5}{2}$	1957/168 000	0.035
1-1-2	0	−1/40	−0.077	$\frac{3}{2}$-$\frac{3}{2}$-$\frac{3}{2}$	0	4/25	0.414
	$\frac{1}{2}$	−1/120	−0.025		$\frac{1}{2}$	1/10	0.273
	$\frac{3}{2}$	−37/6000	−0.019		$\frac{3}{2}$	27/625	0.124
	$\frac{5}{2}$	−349/63 000	−0.017		$\frac{5}{2}$	1957/52 500	0.108

For cascades (a)–(i) listed above, the maximum detector half-angle Θ has been plotted in Fig. 3 as a function of the polarizer efficiency ϵ. This relationship is obtained by using the equality in Eq. (47). $F(\Theta)$ for case (j) is almost identical to that for case (c) and therefore has not been included in Fig. 3. Of particular interest is case (d) since it allows particularly large solid angles with low polarizer efficiency.

Many other variations of initial-state populations are of course possible. Some of these are also included in Table I. Many are redundant. For example, the $(\frac{1}{2}\text{-}\frac{3}{2}\text{-}\frac{3}{2})$ or $(\frac{1}{2}\text{-}\frac{3}{2}\text{-}\frac{1}{2})$ cascades with $P(\frac{1}{2},\frac{1}{2})=1$, $P(\frac{1}{2},-\frac{1}{2})=0$ give results identical to that for the respective cascades with isotropic populations in the initial states. The latter of these, of course, does not satisfy Eq. (48) in any case. The (1-1-0) cascade with $P(1,1)=P(1,0)=1$; $P(1,-1)=0$ satisfies Eq. (48) but offers no advantages over case (d) considered above.

B. Effective Quantum Efficiencies

The normal quantum efficiency specified by photomultiplier-tube manufacturers is the average number of photoelectrons emitted from the photocathode per incident photon. In applications, the quantity of interest is the total detector quantum efficiency p including electron optics—i.e., the average number of current pulses obtained from the photomultiplier per incident photon. This latter quantity can be determined in experiments involving coincidence detection of cascade photons. It differs significantly from the photocathode quantum efficiency.[6,16]

Consider a coincidence experiment in which the initial states are isotropically populated, the angle between the detectors is $\theta_s=\pi$, there are no polarizers, and the detectors subtend cones of half-angles Θ_1 and Θ_2. From Eq. (36) the coincidence rate is

$$S(\Theta_1,\Theta_2)\propto G(\Theta_1)G(\Theta_2)+4AH(\Theta_1)H(\Theta_2). \qquad (49)$$

An analogous result for nuclear γ rays has been obtained by Rose.[17] If the detectors have uniform sensitivity, $s(\theta)=1$, then the maximum fraction of the coincidences which can be observed due to solid-angle limitations is

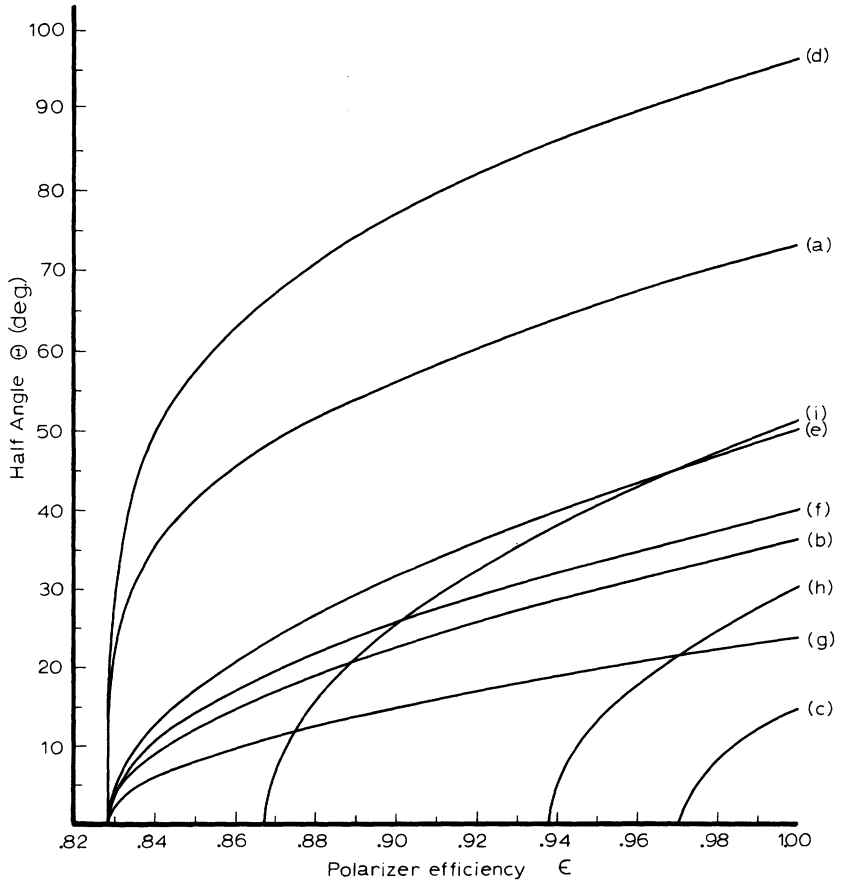

FIG. 3. Maximum values of the detector half-angles vs ϵ for a valid test of local hidden variables. All transitions have zero nuclear spin. They are
(a) 0-1-0;
(b) 0-1-1 or 1-1-0 with isotropic initial populations;
(c) $\frac{3}{2}\text{-}\frac{3}{2}\text{-}\frac{1}{2}$ with isotropic initial populations or $\frac{1}{2}\text{-}\frac{3}{2}\text{-}\frac{3}{2}$ with any initial populations;
(d) 1-1-0 with $P(1,\pm1)=0$, $P(1,0)=1$;
(e) 1-1-1 with $P(1,\pm1)=0$, $P(1,0)=1$;
(f) 1-2-1 with $P(1,\pm1)=0$, $P(1,0)=1$;
(g) 2-1-0 with $P(2,\pm2)=0$, $P(2,\pm1)=3$, $P(2,0)=4$;
(h) 2-2-1 with $P(2,\pm2)=0$, $P(2,\pm1)=3$, $P(2,0)=4$;
(i) $\frac{3}{2}\text{-}\frac{3}{2}\text{-}\frac{1}{2}$ with $P(\frac{3}{2},\pm\frac{3}{2})=0$, $P(\frac{3}{2},\pm\frac{1}{2})=1$.

$$\eta = S(\Theta_1, \Theta_2)/S(\pi, \pi)$$
$$= \tfrac{1}{4}(1 - \cos\Theta_1)(1 - \cos\Theta_2)$$
$$+ \tfrac{1}{16} A \sin^2\Theta_1 \sin^2\Theta_2 \cos\Theta_1 \cos\Theta_2. \quad (50)$$

The first term is the solid-angle fraction for isotropic emissions and the second term gives the anisotropic correction. Depending on the particular transition (the value of A), this correction may be zero or as large as 50% of the isotropic term.

If in the source there are N atoms per second decaying via the cascade, then the number of true coincidences per second observed is

$$N_c = \eta p_1 p_2 N, \quad (51)$$

where p_i is the effective quantum efficiency of the ith detector. Light losses in the filters and other optics are neglected; they may be included by a trivial extension of the discussion. The number of detected photons which are from the first transition in the cascade is

$$N_1 = \tfrac{1}{2}(1 - \cos\Theta_1) p_1 N, \quad (52)$$

since they are emitted isotropically. The effective quantum efficiency of the second detector is then found from Eqs. (51) and (52);

$$p_2 = (1 - \cos\Theta_1)(N_c/2\eta N_1). \quad (53)$$

Thus, p_2 can be determined from measurements of N_1, N_c, Θ_1, and Θ_2.

The effective quantum efficiency of the first detector can also be determined provided the only excited atoms in the source which decay to the intermediate state of the cascade are those in the initial state of the cascade being considered. Since the photons from the second transition in the cascade are emitted isotropically, when considered alone, the number of them detected is

$$N_2 = \tfrac{1}{2}(1 - \cos\Theta_2) p_2 r N, \quad (54)$$

where r is the branching ratio for the decay from the intermediate state being investigated. Hence, we have

$$r p_1 = (1 - \cos\Theta_2)(N_c/2\eta N_2). \quad (55)$$

If r is known, p_1 can be determined and vice-versa. If neither p_1 nor r is known, measurements must be made for all cascades ending in the final state to which the given intermediate state can decay. These results together with the normalization condition on the r's provide sufficient information to determine both p_1 and the branching ratios.

C. Resonance Fluorescence

The derivation of Eq. (1) and the subsequent results, Eqs. (29) and (36), are couched in terms of a cascade in which both radiations are emitted. However, these results apply if the first radiation is absorbed rather than emitted, since the same matrix elements are involved. This process in which the first radiation is absorbed and the second emitted is known as resonance fluorescence. There is, of course, no requirement that the wavelengths of the absorbed and emitted photons be the same.

In such applications the angle Θ_1 is the half-angle of the convergent cone of incident light, and the coincidence rate S becomes the intensity of the emitted radiation. In typical experiments the initial states are isotropically populated, and $\theta_s = \frac{1}{2}\pi$. The intensity of the emitted radiation is then

$$S \propto 3a_1a_2 G(\Theta_1) G(\Theta_2)$$
$$- A[6a_1a_2 H(\Theta_1) H(\Theta_2) - 6a_1b_2 H(\Theta_1) J(\Theta_2) \cos 2\Phi_2$$
$$- 6b_1a_2 J(\Theta_1) H(\Theta_2) \cos 2\Phi_1$$
$$- 2b_1b_2 J(\Theta_1) J(\Theta_2) \cos 2\Phi_1 \cos 2\Phi_2]. \quad (56)$$

This result gives the linear polarization dependences in a 90° resonance fluorescence experiment, including the effects of finite detector and lamp apertures. It gives, for example, the "net fluorescence at zero field" observed experimentally[18] in a 0-1-0 transition.

IV. SUMMARY

The polarization correlation between photons in an atomic cascade has been derived and evaluated. Hyperfine-structure effects have been considered for the first time. The formal expression, Eq. (1), has been evaluated by splitting it into factors depending only on the atomic transitions and factors depending only on the experimental geometry. The former have been put in a simple form and results are tabulated for a broad range of useful atomic transitions and nuclear spins. This includes most transitions which might be experimentally observed. The latter factors were calculated taking into account linear polarizers, arbitrary detector positions, and finite-size detectors with circular apertures. Inconsistencies in the literature regarding the choice of the circular polarization convention have been pointed out. Initial-state populations which are anisotropic are considered when these populations are defined with respect to the laboratory z axis and when one of the detectors lies on this z axis. The final result which we have obtained, Eq. (20) or (36), is needed whenever experimentally realistic predictions are desired for two successive dipole

transitions.

It has been shown that hyperfine-structure effects will render a cascade unsuitable for experimental hidden-variable tests of the type described by Clauser *et al.*[2] It has also been shown that a 1-1-0 transition with zero nuclear spin and the appropriate initial-state populations is particularly suitable for such experiments. The advantage is that the detector solid angles which it allows are significantly larger than those of the transitions originally proposed for such a test.

Finally, a prescription for the determination of the effective quantum efficiency of a photon counting device has been given. This also includes determination of the branching ratios for the various transitions from an excited state.

ACKNOWLEDGMENTS

The author wishes to thank G. D. Doolen and J. H. McGuire for several helpful discussions and for their comments on the manuscript.

APPENDIX A: DERIVATION OF THE FORMAL RESULT FOR TWO-PHOTON CORRELATIONS

The derivation leading to Eq. (1) is outlined briefly in this appendix. The initial state of the atomic system is described by a diagonal density matrix ρ_a. After the cascade the system consists of the atom and two photons and is described by the density matrix

$$\rho_b = H_2 H_1 \rho_a H_1^\dagger H_2^\dagger , \tag{57}$$

where H_1 and H_2 are, respectively, the transition operator for the emission of the first and the second photon.

Suitable basis vectors for describing the initial, intermediate, and final states of the atom are z-component angular momentum eigenstates $|J_i F_i m_i\rangle$, $|JFm\rangle$, $|J_f F_f m_f\rangle$, respectively. Here m is the magnetic quantum number in the F representation. Suitable basis vectors for the first and second photons emitted are plane waves of definite helicity, $|\vec{k}_1\sigma_1\rangle$ and $|\vec{k}_2\sigma_2\rangle$. With these basis vectors the matrix elements of ρ_b are

$$\begin{aligned}\langle f|\rho_b|f'\rangle &= \langle J_f F_f m_f k_2\sigma_2 k_1\sigma_1|\rho_b|J_f F_f' m_f' k_2\sigma_2' k_1\sigma_1'\rangle \\ &= \sum_{\substack{F,F',m,m' \\ F_i,m_i}} [\langle J_f F_f m_f k_2\sigma_2 | H_2 | JFm\rangle \langle JFmk_1\sigma_1 | H_1 | J_i F_i m_i\rangle \langle J_i F_i m_i|\rho_a| J_i F_i m_i\rangle \\ &\quad \times \langle J_i F_i m_i| H_1^\dagger | JF'm'k_1\sigma_1'\rangle \langle JF'm'| H_2^\dagger | J_f F_f' m_f' k_2\sigma_2'\rangle] . \end{aligned} \tag{58}$$

Of the five matrix elements in Eq. (58), the third represents the relative populations in the initial states, i.e., the diagonal elements of the initial density matrix, $P(F_i, m_i)$. The other four have the same form. Consider a typical one $\langle JFmk_1\sigma_1 | H_1 | J_i F_i m_i\rangle$. The operator H_1 is a zero-rank tensor which is the contraction of two first-rank tensors $T_{L,m}$ and $A_{L,m}$. These refer to the atom and to the radiation field, respectively. Thus the matrix element becomes

$$\begin{aligned}&\langle JFmk_1\sigma_1 | H_1 | J_i F_i m_i\rangle \\ &\quad = \sum_M (-1)^M \langle JFm|T_{1M}| J_i F_i m_i\rangle \langle k_1\sigma_1 | A_{1,-M}|\text{vac}\rangle ,\end{aligned} \tag{59}$$

where L has been set equal to unity since only electric dipole transitions are being considered. Applying the Wigner-Eckart theorem to the first of these matrix elements gives

$$\begin{aligned}&\langle JFm| T_{1,M}| J_i F_i m_i\rangle \\ &\quad = (-1)^{m_i - m + F_i + F} [(2F+1)/(2F_i+1)]^{1/2} \\ &\quad \times C(F1F_i;\, m, m_i - m)\, \langle JF||T_1||J_i F_i\rangle ,\end{aligned} \tag{60}$$

where we have set $M = m_i - m$ as required by the Clebsch-Gordan coefficient. Removing the F dependence from the reduced matrix element using $\vec{F} = \vec{I} + \vec{J}$ gives

$$\begin{aligned}&\langle JFm|T_{1,M}| J_i F_i m_i\rangle \\ &\quad \propto (-1)^{m_i - m + F} (2F+1)^{1/2} C(F1F_i;\, m, m_i - m) \\ &\quad \times W(J_i J F_i F;\, 1I).\end{aligned} \tag{61}$$

Now consider the second of the matrix elements on the right-hand side of Eq. (59),

$$\begin{aligned}&\langle k_1\sigma_1 | A_{1,-M}|\text{vac}\rangle \\ &\quad = \sum_{M'} \langle k_1\sigma_1 | 1M'\rangle \langle 1M'| A_{1,m-m_i}|\text{vac}\rangle ,\end{aligned} \tag{62}$$

where the plane-wave state $\langle k_1\sigma_1|$ has been expanded in angular momentum states $\langle LM'|$ with $L = 1$ for dipole radiation. The functions $\langle k_1\sigma_1|1M'\rangle$ are particularly simple if the z axis of quantization coincides with $\vec{k}_1$. Denoting such functions by $\langle 0\sigma_1|1u\rangle$, the connection between the two is given by

$$\langle k_1\sigma_1|1M'\rangle = \sum_u \langle 0\sigma_1|1u\rangle D^1_{u,M'}(\vec{k}_1 \to \vec{z}), \tag{63}$$

where the argument $(\vec{k}_1 \to \vec{z})$ of the rotation matrix

D stands for the Euler angles describing the rotation that carries the propagation direction $\vec{k}_1$ onto the laboratory z axis. If the convention chosen for right and left circularly polarized basis states is, respectively, $\mp(\hat{e}_x \pm i\hat{e}_y)/2^{1/2}$, where $\hat{e}_x$ and $\hat{e}_y$ are unit vectors along the x and y axes, then we have

$$\langle 0\sigma_1|1u\rangle \propto \delta_{\sigma_1,u}. \tag{64}$$

Since the second factor on the right-hand side of Eq. (62) is

$$\langle 1M'|A_{1,m-m_i}|\text{vac}\rangle \propto \delta_{M',m-m_i}, \tag{65}$$

we find by using Eqs. (63) and (64) that the radiation matrix element is

$$\langle k_1\sigma_1|A_{1,-M}|\text{vac}\rangle \propto D^1_{\sigma_1,m-m_i}(\vec{k}_1 \to \vec{z}). \tag{66}$$

Thus the typical matrix element, Eq. (59), is

$$\langle JFmk_1\sigma_1|H_1|J_iF_im_i\rangle \propto (-1)^F(2F+1)^{1/2}C(F1F_i;m,m_i-m) \times W(J_iJF_iF;1I)D^1_{\sigma_1,m-m_i}(\vec{k}_1 \to \vec{z}). \tag{67}$$

The remaining matrix elements in Eq. (58) are obtained analogously. The elements of the final density matrix are therefore

$$\langle f|\rho_b|f'\rangle \propto \sum_{\substack{F,F',m,m'\\F_i,m_i}} [(-1)^{m+m'}P(F_i,m_i)(2F+1)(2F'+1)C(F1F_i;m,m_i-m)C(F'1F_i;m',m_i-m') \times C(F1F_f;m,m_f-m)C(F'1F'_f;m',m'_f-m')W(J_iJF_iF;1I)W(J_iJF_iF';1I) \times W(J_fJF_fF;1I)W(J_fJF'_fF';1I) \times D^1_{\sigma_1,m_i-m}(k_1\to z)D^{1*}_{\sigma'_1,m_i-m'}(k_1\to z)D^1_{\sigma_2,m-m_f}(k_2\to z)D^{1*}_{\sigma'_2,m'-m'_f}]. \tag{68}$$

In the above result the sum over the intermediate-state F values is coherent. When the natural width of the atomic states is much less than the hyperfine-structure splittings this sum must be incoherent. The incoherent sum is obtained by setting $F'=F$ and dropping the sum over F'.

The coincidence rate is given by

$$\text{Tr}\{\epsilon(1)\epsilon(2)\rho_b\} = \sum_f \langle f|\epsilon(1)\epsilon(2)\rho_b|f\rangle = \sum_{f,f'}\langle f|\epsilon(1)\epsilon(2)|f'\rangle\langle f'|\rho_b|f\rangle = \int d\Omega_1 \int d\Omega_2 \sum_{\sigma_1,\sigma'_1,\sigma_2,\sigma'_2}\langle\sigma'_1|\epsilon(1)|\sigma_1\rangle\langle\sigma'_2|\epsilon(2)|\sigma_2\rangle \sum_{F_f,m_f}\langle J_fF_fm_fk_2\sigma_2k_1\sigma_1|\rho_b|J_fF_fm_fk_2\sigma'_2k_1\sigma'_1\rangle. \tag{69}$$

where $\epsilon(1)$ and $\epsilon(2)$ are, respectively, the polarizer efficiency matrices for the first and second emissions. The last matrix element in Eq. (69) is just the result given by Eq. (68) but with the primes dropped from m'_f and F'_f. Finally, Eq. (1) is just Eq. (69) with the incoherent sum over the intermediate-state F values.

APPENDIX B: REDUCTION OF THE COHERENT SUM OVER INTERMEDIATE-STATE F VALUES TO THE $I=0$ RESULT

When the hyperfine-structure splittings are much less than the natural width of the state, a coherent sum over the intermediate-state F values is required in the derivation of the coincidence rate. Such a sum when $I\neq 0$ is identical to that for $I=0$. This can be shown by examining the B coefficients. Consider B_1 first; the argument for the other B coefficients is analogous. With isotropic populations in the initial state and a coherent sum over F, we find from Eqs. (68) and (69)

$$B_1^c = (2I+1)^{-1}\sum_{F_iF_fFF'}(2F+1)(2F'+1)W(J_fJF_fF;1I) \times W(J_fJF_fF';1I)W(J_iJF_iF;1I) \times \sum_{m=-F}^{+F}C(F1F_f;m,1)C(F'1F_f;m,1) \times C(F1F_i;m,-1)C(F'1F_i;m,-1), \tag{70}$$

where we have taken $P(F_i,m_i)=(2I+1)^{-1}$, explicitly including the I dependence of the diagonal elements of the initial density matrix. Following the same procedure that led to Eq. (33), we find

$$B_1^c = (2I+1)^{-1}\sum_{FF'r}(2F+1)(2F'+1)W(1rJ_fJ;1J) \times W(1rJ;J_i1J)W^2(F'FJJ;rI) \times C(11r;1,-1)C(11r;-1,1). \tag{71}$$

Evaluating the sum over F' by using the orthonormality relation for the Racah coefficients and

then completing the sum over F gives

$$B_1^c = \sum_{r=0}^{2} W(1rJ_fJ;\,1J)\,W(1rJ_iJ;\,1J) \times C(11r;\,1,-1)\,C(11r;\,-1,1). \quad (72)$$

Now, the expression for $\overline{B}_1$ when the sum over F is incoherent is

$$\overline{B}_1 = (2I+1)^{-1}\sum_{r=0}^{2}\sum_{F}(2F+1)^2\,W(1rJ_fJ;\,1J) \times W(1rJ_iJ;\,1J)\,W^2(FFJJ;\,rI)\,C(11r;\,1,-1) \times C(11r;\,-1,1). \quad (73)$$

Here the I dependence from the initial density matrix has been explicitly included in the B's. Evaluating Eq. (73) at $I=0$ gives

$$\overline{B}_1(I=0) = \sum_{r=0}^{2} W(1rJ_fJ;\,1J)\,W(1rJ_iJ;\,1J) \times C(11r;1,-1)\,C(11r;\,-1,1). \quad (74)$$

Comparing Eqs. (72) and (74), we see that B_1^c is identical to $\overline{B}_1(I=0)$. Similarly, we find $B_5^c = \overline{B}_5(I=0)$ and $B_9^c = \overline{B}_9(I=0)$. Hence, if the hyperfine-structure splittings are much less than the natural widths of the states, then hyperfine structure has no effect on the coincidence rate.

---

*Work supported by the Robert A. Welch Foundation.

[1]R. D. Kaul, J. Opt. Soc. Am. **56,** 1262 (1966).
[2]J. F. Clauser, M. A. Horne, A. Shimony, and R. A. Holt, Phys. Rev. Lett. **23,** 880 (1969).
[3]L. Bradley III, Phys. Rev. **102,** 293 (1956).
[4]P. L. Sagalyn, Phys. Rev. **102,** 293 (1956).
[5]C. A. Kocher and E. D. Commins, Phys. Rev. Lett. **18,** 575 (1967).
[6]C. Camhy-Val and A. M. Dumont, Astron. Astrophys. **6,** 27 (1970).
[7]S. J. Freedman and J. F. Clauser, Phys. Rev. Lett. **28,** 938 (1972).
[8]S. Devons and L. J. B. Goldfarb, in *Encyclopedia of Physics*, edited by S. Flügge (Springer, Berlin, 1957), Vol. 42, p. 362.
[9]H. Frauenfelder and R. M. Steffen, in *Alpha-, Beta-, and Gamma-Ray Spectroscopy,* edited by K. Siegbahn (North-Holland, Amsterdam, 1966), Vol. 2, p. 997.
[10]M. Horne, Ph.D. thesis (Boston University, 1970) (unpublished).
[11]R. A. Holt (private communication).
[12]Choice of a different convention can lead to the appearance of a factor $\sigma_1\sigma_1'\sigma_2\sigma_2'$ in S, such as appears in Horne's result, Ref. 10.
[13]There is some confusion in the literature in this regard. Compare, for example, the efficiency matrices and the values of $\langle 0\sigma|1M\rangle$ given in Refs. 9 and 10.
[14]M. E. Rose, *Elementary Theory of Angular Momentum* (Wiley, New York, 1957).
[15]B. A. Lippman, Phys. Rev. **81,** 162 (1951).
[16]J. F. Clauser, Lawrence Berkeley Laboratory Report No. LBL967, 1972 (unpublished).
[17]M. E. Rose, Phys. Rev. **91,** 610 (1953).
[18]W. L. Williams and E. S. Fry, Phys. Rev. **183,** 81 (1969).